

Breakthrough curves and elution profiles of single solutes in case of adsorption isotherms with two inflection points

Weibing Zhang^{a,b}, Yichu Shan^a, Andreas Seidel-Morgenstern^{a,c,*}

^a *Max-Planck-Institut für Dynamik komplexer technischer Systeme, Sandtorstrasse 1, D-39106 Magdeburg, Germany*

^b *Dalian Institute of Chemical Physics, Chinese Academy of Sciences, Dalian 116011, China*

^c *Otto-von-Guericke-Universität, für Verfahrenstechnik, Universitätsplatz 2, D-39106 Magdeburg, Germany*

Received 12 October 2005; received in revised form 12 December 2005; accepted 20 December 2005

Available online 24 January 2006

Abstract

The shape of breakthrough curves and elution profiles depends strongly on the course of the specific equilibrium functions characterizing the chromatographic system. For a highly efficient system the equilibrium theory provides a methodology how to predict the band profiles. The concept is frequently applied to analyze single component systems characterized by isotherms possessing simple shapes (Langmuir or anti-Langmuir behaviour). However, adsorption isotherms often possess more complicated shapes and have inflection points in their courses. This leads to the development of composite concentration waves and results in complex shapes of breakthrough curves and elution profiles. In this paper, the equilibrium theory is used to predict breakthrough curves for a chromatographic system characterized by an adsorption isotherm with two inflection points. The results obtained are validated by comparing with numerical solutions of the equilibrium dispersive model.

© 2006 Elsevier B.V. All rights reserved.

Keywords: Equilibrium theory; Adsorption isotherms; Inflection points; Breakthrough curves

1. Introduction

There are several models available which are capable to predict elution profiles for chromatographic processes under overloaded conditions [1,2]. In general these models take into account the distribution equilibria and, in different detail, mass transfer resistances. Typically the corresponding balance equations must be solved numerically. Instructive analytical solutions can be derived using the equilibrium theory of chromatography which neglects all mass transfer limitations [3–5]. These solutions describe essential features of the development of concentration profiles in chromatographic columns.

In order to apply the equilibrium theory to describe chromatographic processes the underlying distribution equilibrium functions must be provided. Under diluted conditions these functions are linear and migration speeds do not depend on concentration.

If larger sample sizes are introduced in a chromatographic column the nonlinear range of the equilibrium functions becomes important and migration speeds depend on concentration. This leads to the formation of compressed and dispersed fronts. The migration speeds and the shapes of the corresponding fronts can be predicted using the equilibrium theory exploiting the method of characteristics [3–9]. The application of the concept is in particular simple and capable to predict the development of the band profile for a single component characterized by an isotherm which is completely convex or concave. Applying elegant coordinate transformations also analytical solutions were derived which describe the behavior of mixtures obeying certain types of competitive adsorption isotherms [3–5]. The powerful concept was further already extended successfully in order to predict the performance of more sophisticated multicolumn arrangements, as e.g. applied in the simulated moving bed process [10,11].

First results regarding the relation between the courses of the isotherms and the shapes of single component elution profiles were reported in [12] for equilibria of the Langmuir or anti-Langmuir type. Later Klamer and Van Krevelen [13] pointed out

* Corresponding author. Tel.: +49 391 67 18643; fax: +49 391 67 12028.
E-mail address: andreas.seidel-morgenstern@vst.uni-magdeburg.de (A. Seidel-Morgenstern).

that adsorption isotherms often possess inflection points. They investigated the chromatographic behavior of a solute characterized by an isotherm with a single inflection point and they briefly illustrated already the complex profiles in case of an adsorption isotherm with two inflection points. Instructive schematic illustrations regarding the impact of inflection points in the course of an adsorption isotherms on the shape of band profiles were provided in [5,6] applying equilibrium theory. However, still there is a lack in explicit demonstrations of this relation using concrete parameters of an isotherm model and a specific chromatographic system.

In this paper, selected aspects of the equilibrium theory will be shortly revised. For illustration simple isotherms (of the Langmuir and anti-Langmuir type) will be used. Then examples of more complex isotherm shapes will be given. An experimental result will be presented to demonstrate the strong correlation between isotherm course and shape of breakthrough curves. In the main part of the paper the equilibrium theory will be applied in order to analyze step responses for a chromatographic system characterized by an adsorption isotherm possessing two inflection points. Finally, results of numerical simulations applying the equilibrium dispersive model will be presented in order to validate the analytical results obtained.

2. Relation between curvatures of adsorption isotherms and shapes of adsorption and desorption fronts

The basis of the equilibrium theory of chromatography is to neglect all kinetic effects causing band broadening and to assume that the distribution equilibrium of a solute between the mobile and stationary phases is permanently established. Thus, the following mass balance equation holds true [1–5]:

$$\frac{\partial c}{\partial t} + F \frac{\partial q(c)}{\partial t} + u \frac{\partial c}{\partial x} = 0 \quad (1)$$

In the above, c and q are the concentrations in the mobile and stationary phases and F is the phase ratio for which holds $F = (1 - \varepsilon)/\varepsilon$ with ε being the total column porosity. In Eq. (1) the mobile phase velocity u is assumed to be constant as it is typically the case in liquid chromatography.

The solution of Eq. (1) requires the specification of initial and boundary conditions. Typically is assumed a fixed-bed uniformly preloaded with an initial concentration c^{Init} and a rectangular injection profile introduced between $t = 0$ and $t = t^{\text{inj}}$:

$$c(t = 0, x) = c^{\text{Init}} \quad (2)$$

$$c(t, x = 0) = \begin{cases} c^{\text{inj}} & \text{for } 0 < t \leq t^{\text{inj}} \\ c^{\text{Init}} & \text{for } t^{\text{inj}} < t \end{cases} \quad (3)$$

If the injection time t^{inj} is large enough the whole fixed-bed is completely transformed from the first equilibrium state corresponding to the initial condition ($c^{\text{Init}}, q(c^{\text{Init}})$) into a new equilibrium state corresponding to the injection concentration ($c^{\text{inj}}, q(c^{\text{inj}})$). This problem is the classical and extensively studied Riemann problem [5]. Exploiting the method of characteristics there is a complete theory available providing the solution of Eq. (1) and discussing its properties [3–5]. The shape of the resulting

breakthrough curves depends (a) on the direction of the process (adsorption for $c^{\text{Init}} < c^{\text{inj}}$, desorption for $c^{\text{Init}} > c^{\text{inj}}$) and (b) on the shape of the isotherm.

In case of nonlinear isotherms compressed fronts (shocks) or dispersed front (waves) propagate through the fixed-bed with characteristic velocities. Hereby the velocity of a shock is related to the isotherm chord between the two limiting concentrations before (c^-) and after (c^+) the shock according to:

$$u_{\text{shock}}(c^-, c^+) = \frac{u}{1 + F((q(c^+) - q(c^-))/(c^+ - c^-))} \quad (4)$$

The velocity in a simple wave depends on concentration according to:

$$u_{\text{wave}}(c^*) = \frac{u}{1 + F(dq(c)/dc)|_{c^*}} \quad (5)$$

Eqs. (1)–(5) have been studied intensively for different simple adsorption isotherm models (e.g. [1–11]). Fig. 1 illustrates for Langmuir and anti-Langmuir systems the close relation between the curvature of the isotherm and the shape of adsorption and desorption fronts. Hereby an important and general rule is the fact that operating lines for an adsorption step ($c^{\text{inj}} > c^{\text{Init}}$) or a desorption step ($c^{\text{inj}} < c^{\text{Init}}$) are given by the closest connection between these two concentrations below or above the isotherm. These two operating lines form in mathematical terms the *convex hull* of the isotherm. Thus, the operating lines follow either the slope of the equilibrium function or the chords between two characteristic concentrations. The operating lines can be considered as rubber bands connecting c^{Init} and c^{inj} on both sides of the isotherm [6,14]. Fig. 1 illustrates the well-known fact that for Langmuir the adsorption front systems is sharp whereas the desorption front is disperse. The opposite holds true for anti-Langmuir systems.

3. Isotherms with inflection points and example for corresponding breakthrough curves

Several studies devoted to classify the possible shapes of single component adsorption isotherms have been performed (e.g. [15,16]). Fig. 2 presents the classification of typical adsorption isotherms of dissolved substances given by Giles et al. [16].

Experimental results demonstrating the effect of the isotherm shape on the course of breakthrough curves were given e.g. in [17]. Fig. 3 shows breakthrough curves measured at 20 °C for the (+)-enantiomer of Tröger's base with ethanol as the mobile phase and microcrystalline cellulose triacetate as the stationary phase. The adsorption isotherm is characterized initially by an anti-Langmuir behavior which turns after an inflection point into Langmuir behavior (case I in Fig. 2). As a consequence step responses between $c^{\text{Init}} = 0$ and a feed concentration below the inflection point lead to a dispersed adsorption front and a sharpened desorption front. The opposite holds true if the exchange is performed above the isotherm inflection point as can be seen from the results of the second stages of the staircase experiment. The small initial increase in the detector signal is due to an impurity in the feed solution. Information regarding the range of retention times and more details including a suitable isotherm model is given in [17].

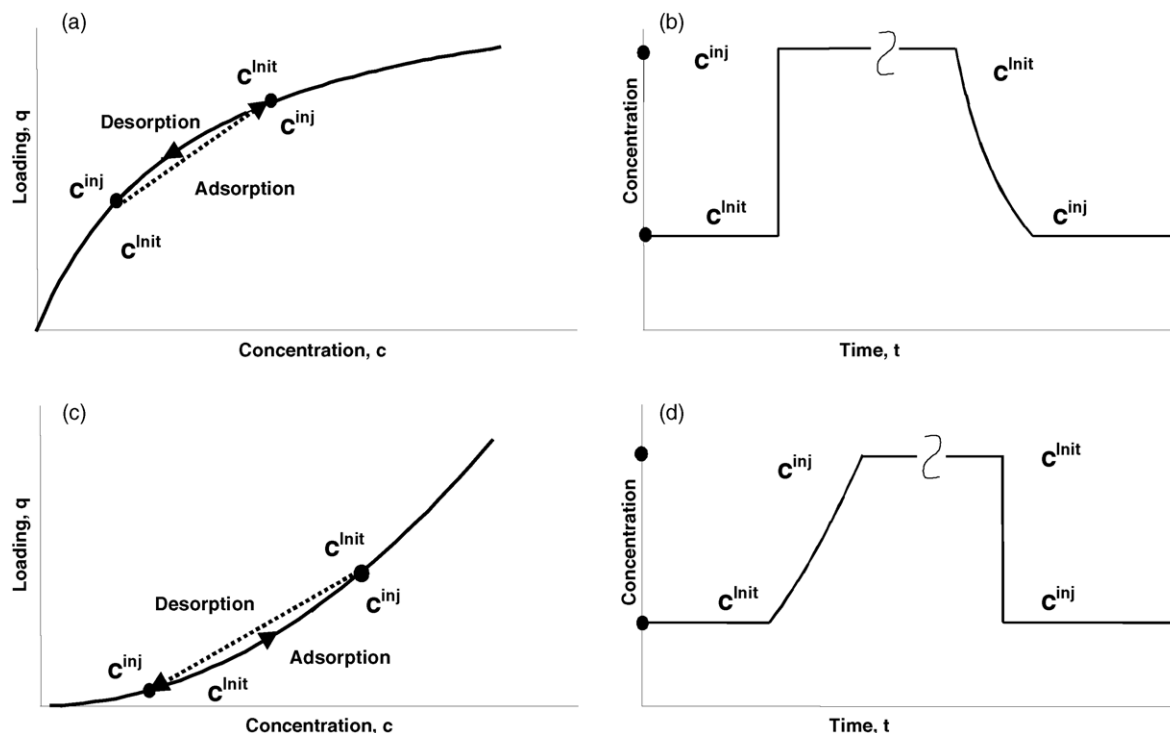


Fig. 1. Illustration of the relation between the shape of the adsorption isotherms (left, fat lines) and the shape of corresponding step response curves. (a) Langmuir isotherm, (b) corresponding sharpended adsorption front and dispersed desorption front, (c) anti-Langmuir isotherm, and (d) corresponding dispersed adsorption front and sharpened desorption front.

Interesting experimental results for an even more complex system characterized by an isotherm with two inflection points was reported in [18].

4. Parameters for case study

The analysis presented below was performed for a situation corresponding to the isotherm type encircled as case II in Fig. 2.

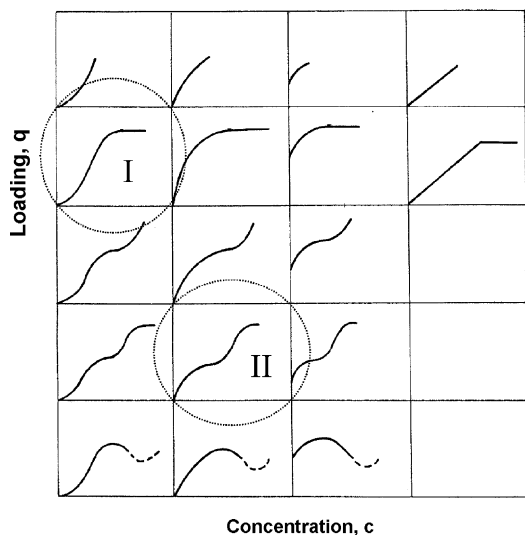


Fig. 2. Typical shapes of the equilibrium functions for single component adsorption from solution (according to Giles et al. [16]). Experimental (I) and theoretical (II) results are given for the two cases encircled.

Thus, the equilibrium function is initially of the Langmuir type and has then two inflection points. Such a case was already discussed in [18,19]. Based on concepts described in [20] the isotherm illustrated in Fig. 1 of [19] was described quantitatively using the following flexible model equation assuming the existence of two different types of adsorption sites on a heterogeneous surface.

$$q = q_{s1}c \frac{b_1 + 2b_2c}{1 + b_1c + b_2c^2} + q_{s2}c \frac{b_3}{1 + b_3c} \quad (6)$$

Using this equation and the five parameters given in Table 1 the isotherm presented in [19] could be well represented. For the goal of this study the physical significance of the parameters of Eq. (6) is of no relevance. Fig. 4 shows the course of the

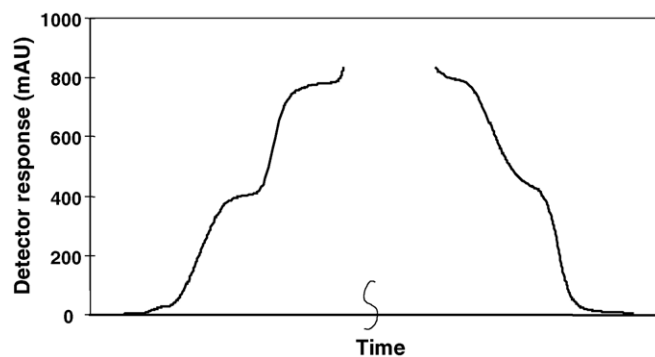


Fig. 3. Experimentally determined step response curves for the (+)-enantiomer of Tröger's base (mobile phase: ethanol, stationary phase: microcrystalline cellulose triacetate, isotherm of case I in Fig. 2) [17].

Table 1
Parameters of analyzed adsorption isotherm (Eq. (6), Fig. 4)

Parameter	Value
q_{s1}	0.84 g/L
q_{s2}	8.83 g/L
b_1	-0.454 L/g
b_2	0.0792 (L/g) ^{0.5}
b_3	3.71 L/g

isotherm, $q(c)$, together with the concentration dependence of the local slopes, dq/dc , and the chords with the origin, q/c . If the liquid concentration is relatively low (between 0 and c_B) or high (above c_E) the branch of the isotherm is of the Langmuir type. The intermediate concentration range (between c_B and c_E) exhibits anti-Langmuir behavior.

In Fig. 4 are marked several characteristic concentrations. B and E mark inflection points of the adsorption isotherm, slope and chord are identical at D, the chord at point H equals to that at point D, the slopes at points A and G are equal, slope and chord are identical at point F. These points are important for the development of the band profiles as will be shown below.

Besides the adsorption isotherm, also geometric parameters of the column, the phase ratio and operating conditions regarding flowrate and injection characteristics must be provided in order to analyze concrete concentration profiles. The reference parameters used in this study are summarized in Table 2. They reflect typical laboratory scale HPLC situations.

5. Breakthrough curves for selected feed concentrations

Below the construction of band profiles will be demonstrated based on the equilibrium theory of chromatography. The adsorption isotherm given in Fig. 4 and different feed concentrations will be considered starting from higher values for c^{inj} going to lower values. The injection time assumed ($t^{inj} = 1.661$ min) is large enough to assure for the situations analyzed that a complete

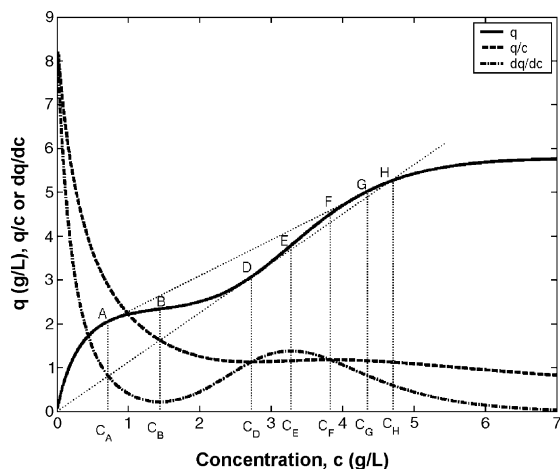


Fig. 4. Courses of an adsorption isotherm with two inflection points (case II in Fig. 2) and the corresponding chords and slopes (according to Eq. (6) with parameters given in Table 1). The liquid phase concentration values of points A, B, D–F, G and H are 0.7098, 1.442, 2.723, 3.279, 3.8285, 4.3457 and 4.653 g/L, respectively.

Table 2
Parameter of the chromatographic system used in conjunction with the isotherm model summarized in Table 1

Column length	$L = 25$ cm
Column diameter	$D = 0.46$ cm
Total porosity	$F = 0.25$ ($\epsilon = 0.80$)
Volumetric flowrate	$\dot{V} = 1$ mL/min
(Mobile phase velocity)	$(u = 7.523$ cm/min)
(Void time)	$(t_0 = 3.322$ min)
Injection volume	$V^{inj} = 1.661$ mL ^a
(Injection time)	$(t^{inj} = 1.661$ min = $t_0/2$)

^a Standard value (used in most calculations).

breakthrough is achieved, i.e. a plateau concentration corresponding to the feed concentration appears at the column outlet.

5.1. $c^{inj} = 5.8$ g/L $> c_H$

According to the “rubber band rule” the operating lines described above, for injection concentrations larger than c_H the adsorption front will travel according to Eq. (4) as a shock with $c^- = 0$ and $c^+ = c^{inj}$ leading to the following shock propagation velocity:

$$u_{shock,0/c^{inj}} = \frac{u}{1 + F(q^{inj}(c^{inj})/c^{inj})} \quad (7)$$

In contrast, the operating line of the desorption front is more complex and consists out of three parts. Between $c = 0$ and c_A and between c_G and c_H simple waves form. The velocity with which in these ranges concentrations propagate is described by Eq. (5). Between c_A ($=c^+$) and c_G (c^-) a shock exists which possesses the following velocity:

$$u_{shock,A/G} = \frac{u}{1 + F((q_G(c_G) - q_A(c_A))/(c_G - c_A))} \quad (8)$$

The development of the band profile in the column is shown in Fig. 5. At three different times are presented the characteristics in time-space-diagrams (where the slopes are the reciprocal velocities of the specific concentrations) and the locations and shapes of the adsorption and desorption fronts inside the column. Whereas in a shock these velocities are the same for all included concentrations, there are individual values in a simple wave. In the plots is also considered the time difference between the start of the adsorption and desorption fronts, i.e. t^{inj} . With proceeding time (from top to bottom) the initially rectangular pulse propagates deeper into the column and changes its shape. The resulting breakthrough curves at the column outlet are shown in Fig. 6 for the adsorption and desorption fronts.

5.2. $c_G < c^{inj} = 4.5$ g/L $< c_H$

If the injection concentration is smaller and falls into segment GH (see Fig. 4), the shape of the profile gets more complex. To understand the development of the adsorption and desorption fronts, the corresponding operating lines are illustrated in Fig. 7.

Now also the adsorption front will split into three parts. Two shocks with (slightly) different velocities will be divided by a

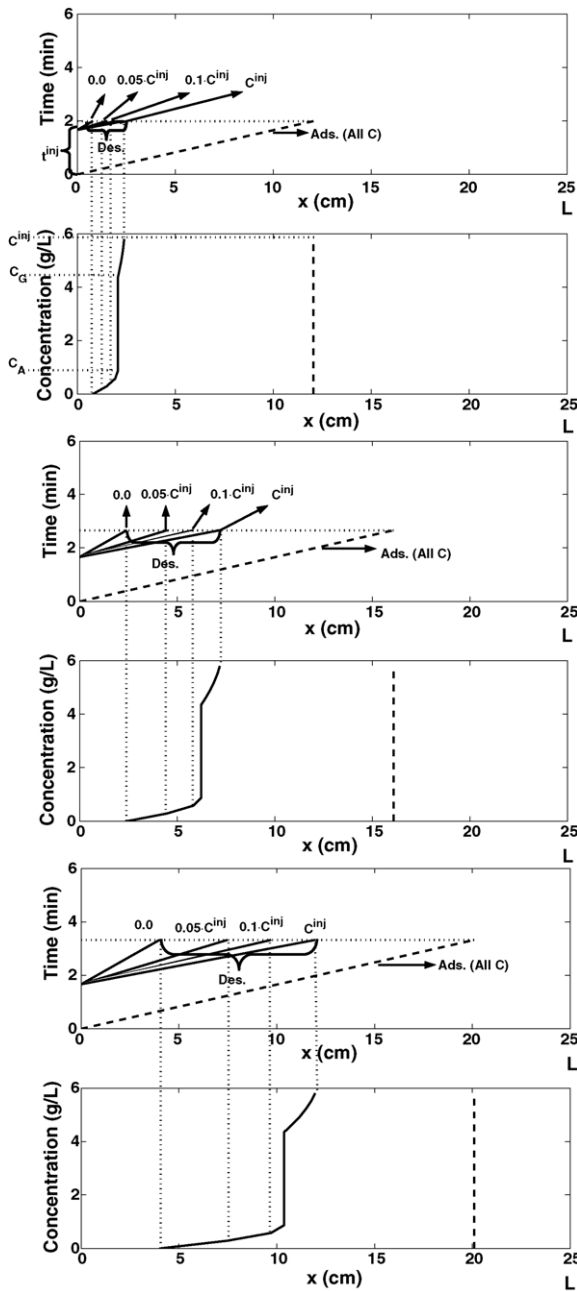


Fig. 5. Illustration of the development of the band profile in the column when the injection concentration is $c^{inj} = 5.8 \text{ g/L}$ (and thus larger than c_H , Fig. 4). The characteristics of the adsorption and desorption fronts and the corresponding internal concentration profiles are shown for three different times ($0.6 \times t_0$; $0.8 \times t_0$ and t_0 , from top to bottom).

(small) wave between c_D and c_Y (Fig. 7). The desorption branch will still consist out of two waves and a shock in between. The high concentration wave exists only in a very small concentration range (between c_G and c^{inj}). All relevant propagation velocities can be again calculated using Eqs. (4) and (5).

Similar to Fig. 5, the development of the band profile in the column at three different times is illustrated in detail in Fig. 8. The resulting concentration profile appearing at the column outlet is given in Fig. 9.

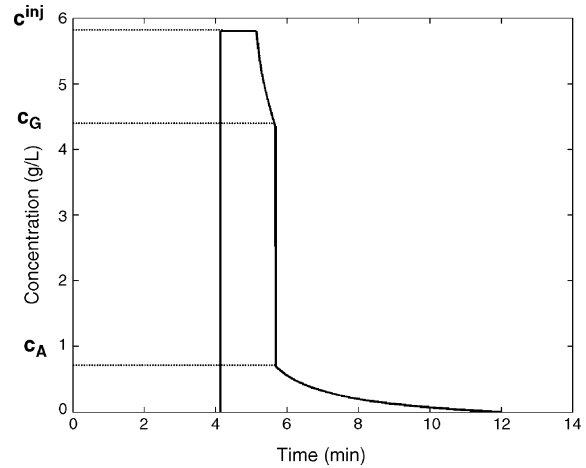


Fig. 6. The elution profile of the solute at the column outlet ($x=L=25 \text{ cm}$) corresponding to Fig. 5 ($c^{inj} = 5.8 \text{ g/L}$).

5.3. $c_E < c^{inj} = 4.0 \text{ g/L} < c_G$

The shape of elution profile for an injection concentration in the segment EG is shown in Fig. 10. In contrast to the previous case (Figs. 7–9) the high concentration wave of the desorption front disappears. The velocity of the shock in the desorption front is not anymore related to c_A but to a (slightly) larger concentration c_I . The difference between the two velocities of the shocks in the adsorption front becomes more pronounced as, consequently, the simple wave between c_D and c_Y . The latter concentration is (slightly) larger compared to Fig. 9.

5.4. $c_D < c^{inj} = 3.0 \text{ g/L} < c_E$

In Fig. 11 is shown the profile at the column outlet for an injection concentration between c_D and c_E . In the adsorption front there is at first a shock between zero and c_D , followed by

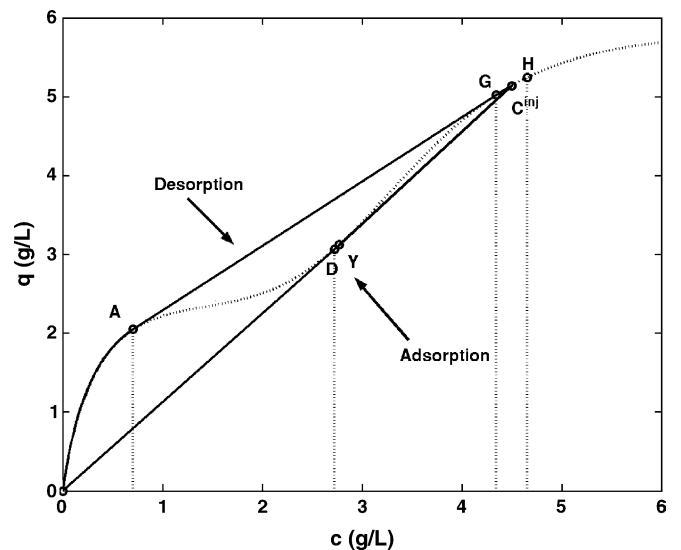


Fig. 7. Illustration of the operating lines (fat) for adsorption (below isotherm) and desorption (above isotherm) for an injection concentration $c^{inj} = 4.5 \text{ g/L}$, i.e. between c_G and c_H (compare with Figs. 1 and 4). The isotherm is shown as dotted line.

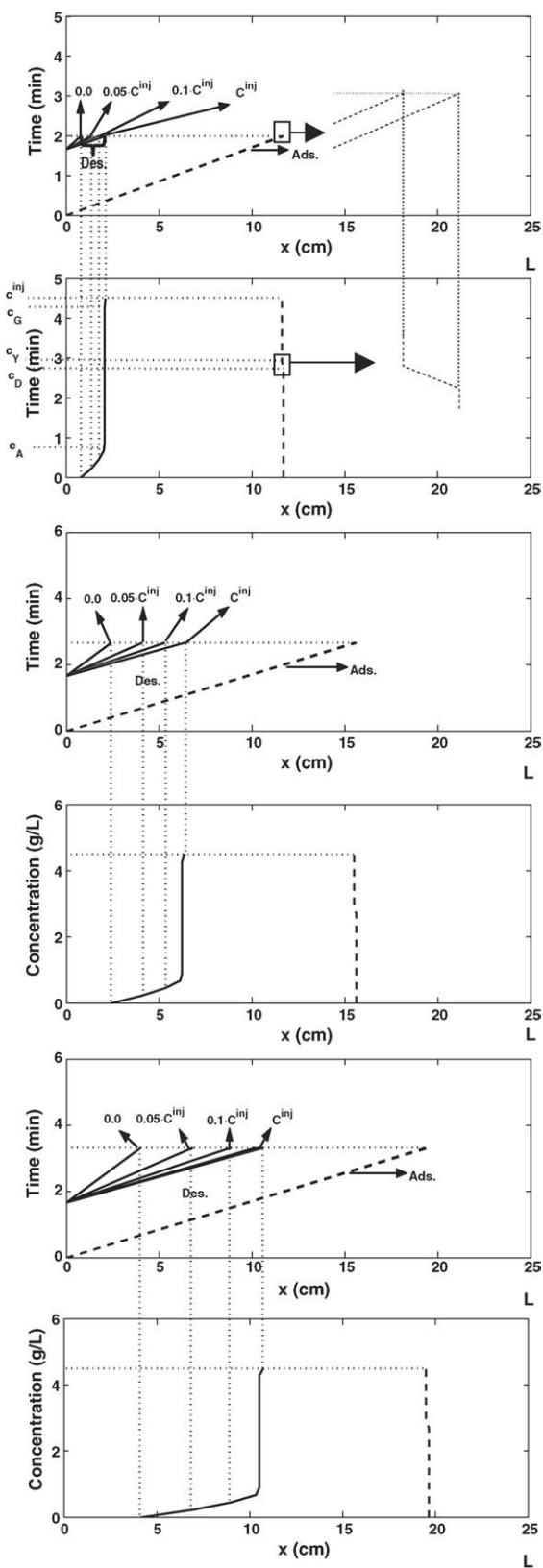


Fig. 8. Development of the band profile in the column when the injection concentration is $c^{inj} = 4.5 \text{ g/L}$ (and thus larger between c_G and c_H , Fig. 4). The characteristics of the adsorption and desorption fronts and the corresponding internal concentration profiles are shown for three different times after the beginning of the injection ($0.6 \times t_0$; $0.8 \times t_0$ and t_0 , from top to bottom).

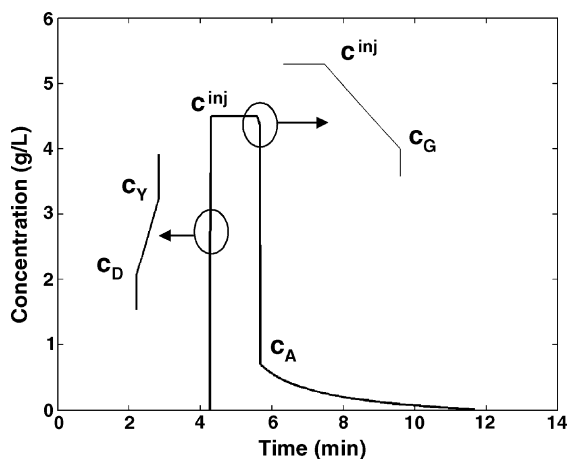


Fig. 9. The elution profile of the solute at the column outlet ($x=L=25 \text{ cm}$) corresponding to Fig. 8 ($c^{inj} = 4.5 \text{ g/L}$).

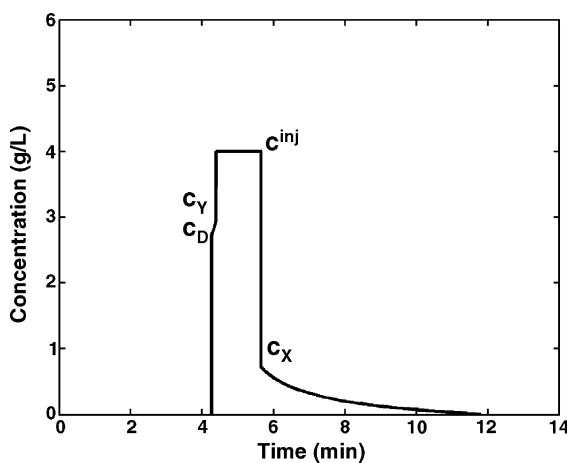


Fig. 10. The elution profile of the solute at the column outlet corresponding to an injection concentration $c^{inj} = 4.0 \text{ g/L}$.

a wave up to the injection concentration. In the desorption front the concentration decreases at first as a shock from the injection concentration to c_{II} followed by a decrease down to zero in a simple wave.

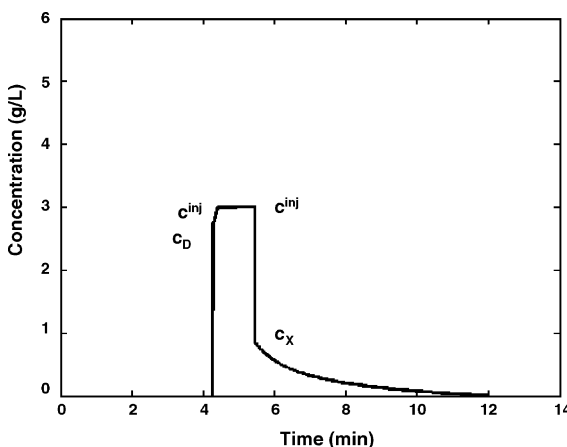


Fig. 11. The elution profile of the solute at the column outlet corresponding to an injection concentration $c^{inj} = 3.0 \text{ g/L}$.

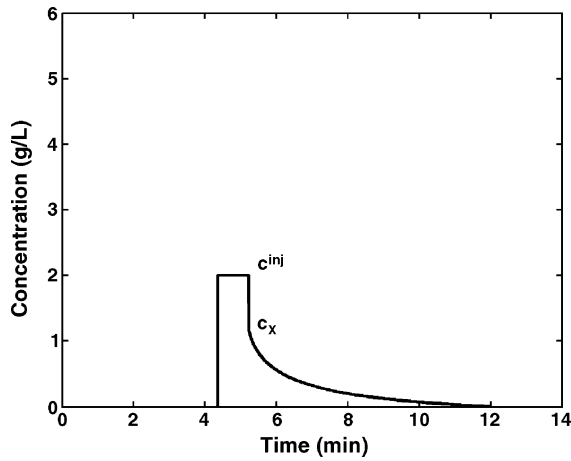


Fig. 12. The elution profile of the solute at the column outlet corresponding to an injection concentration $c^{\text{inj}} = 2.0 \text{ g/L}$.

5.5. $c_B < c^{\text{inj}} = 2.0 \text{ g/L} < c_D$

If the injection concentration drops in the range between points B and D the simple wave in the adsorption front disappears. Compared to the previous case, the velocity of the shock in the desorption front is higher. The shape of the concentration profile as constructed for the column outlet is shown in Fig. 12.

5.6. $c^{\text{inj}} = 1.0 \text{ g/L} < c_B$

Finally, the most simple case is considered which corresponds to the standard Langmuir situation already illustrated in Fig. 1. The profile at the column outlet (Fig. 13) exhibits a single shock for adsorption front. The velocity of this shock is smaller than for the previous situations leading to a larger retention time. The desorption front is characterized by a single simple wave. In Fig. 13, can also be recognized that the sample size injected is just sufficient to reach the injection concentration at the column outlet.

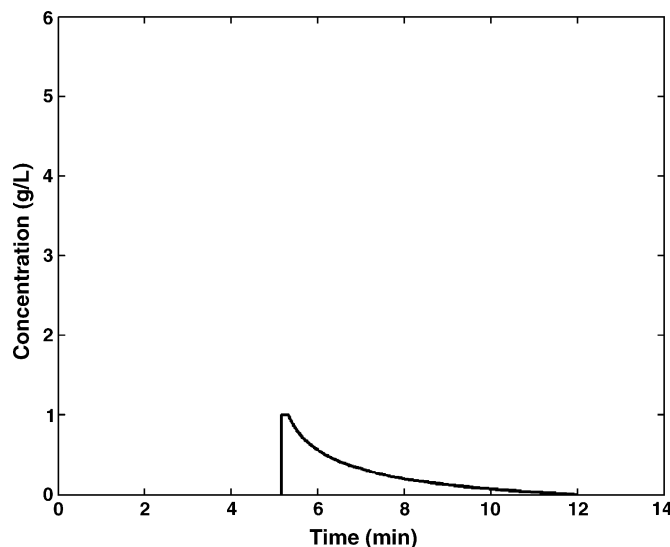


Fig. 13. The elution profile of the solute at the column outlet corresponding to an injection concentration $c^{\text{inj}} = 1.0 \text{ g/L}$.

Smaller injection times would lead to larger retention times of the adsorption fronts and to maximum outlet concentrations below the injection concentration. A limiting situation results for very small sample sizes where low concentrated adsorption and desorption fronts coincide at the analytical retention time, $t_{R,\text{analytical}} = (L/u)(1 + F(q_{s1}b_1 + q_{s2}b_3))$.

6. Numerical validation and simulation of chromatograms

In order to check and evaluate the results obtained by applying the equilibrium theory, additional calculations were carried out using the equilibrium dispersive model.

6.1. Equilibrium dispersive model

The mass balance equation of the equilibrium dispersive model is [1]:

$$\frac{\partial c}{\partial t} + F \frac{\partial q(c)}{\partial t} + u \frac{\partial c}{\partial x} = D_{\text{ap}} \frac{\partial^2 c}{\partial x^2} \quad (9)$$

In contrast to Eq. (1) a dispersion term is added. Into the apparent dispersion coefficient D_{ap} are lumped all band broadening effects. For efficient columns this coefficient is directly related to a finite number of theoretical plates, N , according to:

$$D_{\text{ap}} = \frac{uL}{2N} \quad (10)$$

Eq. (9) was solved using the reliable and efficient explicit finite difference method proposed by Rouchon et al. [1].

6.2. Numerical simulation of elution profiles

Fig. 14 presents for different characteristic injection concentrations and a plate number of $N = 10000$ simulation results

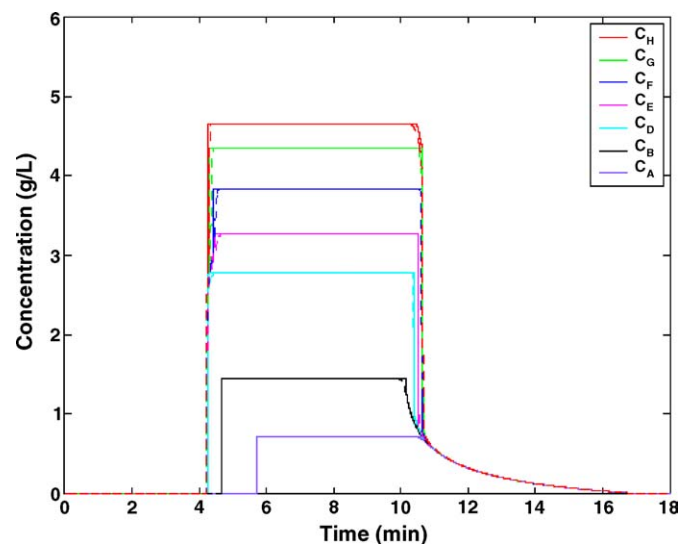


Fig. 14. Comparison between analytical solution of the equilibrium theory (solid lines) and simulated elution profiles calculated with the equilibrium dispersive model (Eq. (9)) and $N = 10,000$ (dashed lines) for different characteristic injection concentrations (Fig. 4) and $t^{\text{inj}} = 2 \times t_0 = 6.644 \text{ min}$.

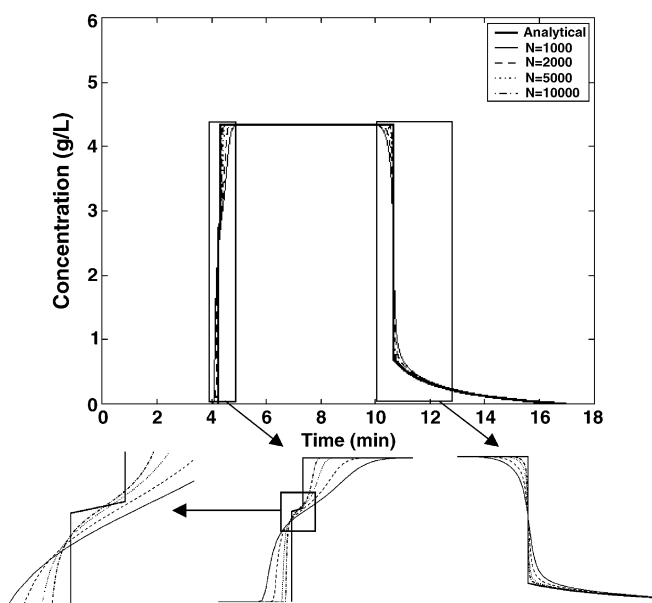


Fig. 15. Comparison between analytical (equilibrium theory) and simulated (equilibrium dispersive model with different plate numbers N) elution profiles for an injection concentration of $c^{inj} = 4.5$ g/L and an injection time of $t^{inj} = 6.644$ min.

obtained with the equilibrium dispersive model. The results are hardly distinguishable from the results provided by the equilibrium theory. Differences can be only identified comparing the perfect shocks predicted by the equilibrium theory and the slightly dispersed fronts predicted by the rate model.

In order to study the influence of the plate number on the convergence of the solution of the rate model into the analytical solution of the equilibrium theory, different values between $N = 1000$ and $N = 10,000$ were used. As for the calculations shown in Figs. 7–9, in Fig. 15 an injection concentration of $c^{inj} = 4.5$ g/L was considered. Obviously there is a gradual convergence of the numerical into the analytical solution for increased plate numbers. However, Fig. 15 also reveals that a plate number even higher than 10,000 would be required to describe properly the positions for the transitions between shocks and simple waves which are predicted by the equilibrium theory.

6.3. Critical Injection time

The above discussion was restricted to situations where the injection time was large enough to assure that the injection concentration was reached at the column outlet. Using the equilibrium theory it is possible to calculate the migration speed of the injection concentration in the adsorption and desorption fronts. Regarding their corresponding retention times at the column outlet ($x = L$) holds:

$$t_{R,ads}(c^{inj}) = \frac{L}{u_{ads}(c^{inj})} \quad (11)$$

$$t_{R,des}(c^{inj}) = \frac{L}{u_{des}(c^{inj}) + t^{inj}} \quad (12)$$

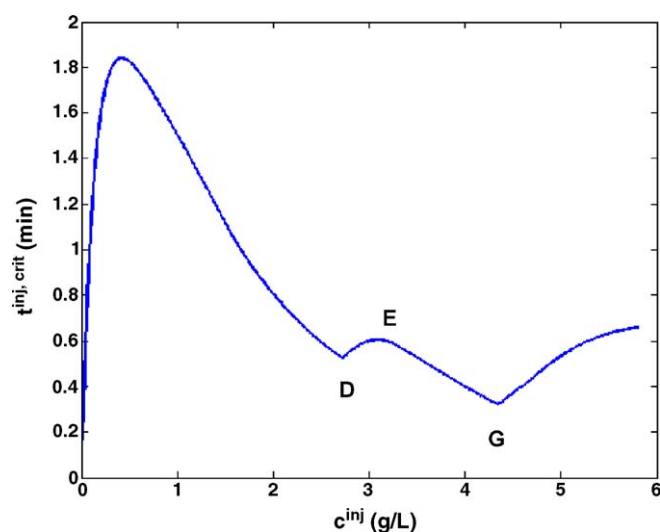


Fig. 16. Dependence of the critical injection time that still assures the survival of the injection concentration at the column outlet (Eq. (13)).

Matching these two times it is possible to calculate a critical injection time according to:

$$t^{inj,crit} = L \left(\frac{1}{u_{ads}(c^{inj})} - \frac{1}{u_{des}(c^{inj})} \right) \quad (13)$$

If for a given injection concentration c^{inj} the injection time is smaller than $t^{inj,crit}$ the maximum concentration of the elution profile at the column outlet will drop below c^{inj} . For the isotherm given in Fig. 4 the dependence $t^{inj,crit}$ versus c^{inj} (Eq. (13)) is shown in Fig. 16. Due to the complex shape of the isotherm a nontrivial dependence results. Fig. 17 shows for $c^{inj} = 0.4$ g/L theoretical concentration profiles in the column according to the equilibrium theory at two different times. Since the used injection time of 1.661 min is smaller than the critical injection time of 1.841 min the maximum outlet concentration is smaller

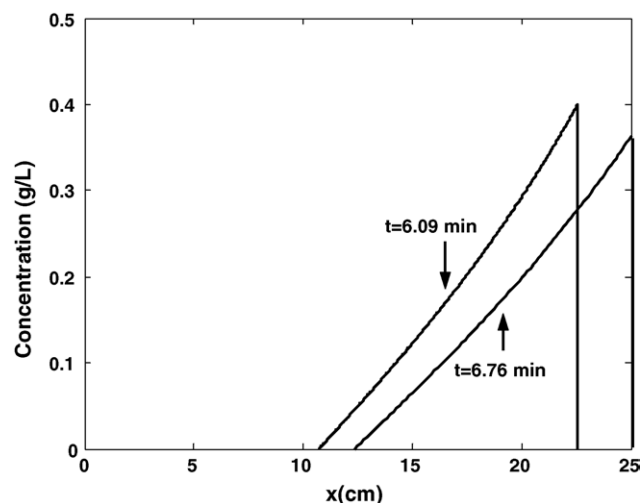


Fig. 17. Band profiles in the column based on equilibrium theory for an injection concentration $c^{inj} = 0.4$ g/L and an injection time $t^{inj} = 1.661$ min which is smaller than the critical time $t^{inj,crit} = 1.841$ min (Eq. (13)). The profiles are given at $t_1 = 6.09$ min where $c^{max} = c^{inj}$ is at $L(t^{inj}/t^{inj,crit}) = 22.56$ cm and at $t_2 = 6.76$ min where $c^{max} = c^{inj}$ is at the column outlet.

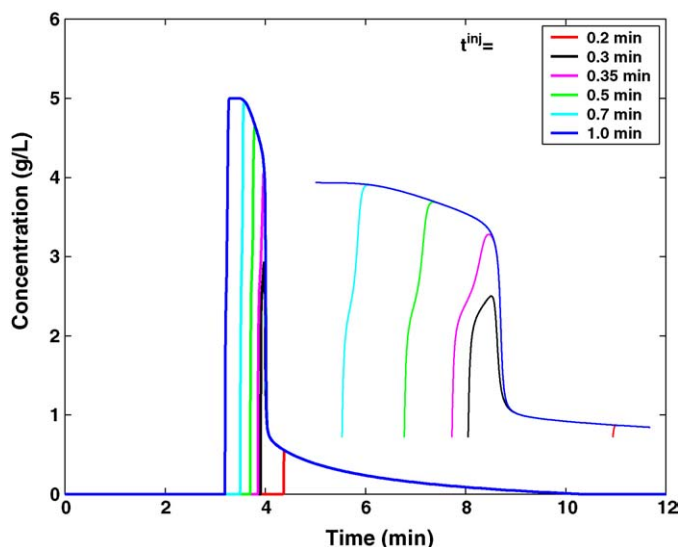


Fig. 18. Elution profiles for $c^{\text{inj}} = 5.0 \text{ g/L}$ ($> c_H$), $N = 10,000$ and different injection times above and below the critical injection time $t^{\text{inj,crit}} = 0.537 \text{ min}$.

than 0.4 g/L . Eq. (13) also allows calculating the last position in the column where the injection concentration is still maintained. The result ($x = 22.56 \text{ cm}$) is illustrated in the figure.

Fig. 18 presents numerical results for $c^{\text{inj}} = 5 \text{ g/L}$ ($> c_H$), $N = 10,000$ and 6 different injection times which are above (1.0 and 0.7 min) and below (0.5, 0.35, 0.3 and 0.2 min) the critical time $t^{\text{inj,crit}} = 0.537 \text{ min}$. The results for $t^{\text{inj}} > t^{\text{inj,crit}}$ are again in good agreement with (not shown) predictions of the equilibrium theory. Due to the limited efficiency already for $t^{\text{inj}} = 0.7 \text{ min}$ the injection concentration is hardly reached at the column outlet. For the cases where $t^{\text{inj}} < t^{\text{inj,crit}}$ the maximum concentrations at the column outlet are smaller than the injection concentration. To predict these profiles using the equilibrium theory the unknown maximum concentration must be determined using additional mass balance considerations which are outside the scope of this paper.

7. Conclusion

The paper demonstrated how the equilibrium theory of chromatography can be applied in order to predict adsorption and desorption fronts in cases where the adsorption isotherms possess inflection points. The analysis was undertaken for a specific isotherm characterized by two inflection points (Langmuir/anti-Langmuir/Langmuir behavior). The development of corresponding elution profiles in the chromatographic column was illustrated for situations where the injection time was sufficient to maintain the feed concentration at the column outlet. Assuming relatively high plate numbers additional numerical calculations were carried out using the equilibrium dispersive model. The results achieved were in good agreement with the analytical solutions provided by the equilibrium theory.

To describe with the equilibrium theory situations where the injection time is not large enough to reach the injection concentration at the column requires future work. An equation to estimate the critical injection time is provided in this paper.

The approach presented can be extended easily to predict breakthrough curves for single solutes possessing other and even more complex isotherm shapes.

Although a real chromatographic system provides only a finite efficiency, quickly accessible predictions provided by the equilibrium theory are considered to be very useful in order to understand the development of band profiles and to design separation processes.

8. Nomenclature

b_1	parameters of adsorption isotherm, Eq. (6) (L/g)
b_2	parameters of adsorption isotherm, Eq. (6) (L/g) ²
b_3	parameters of adsorption isotherm, Eq. (6) (L/g)
c	concentration of solute in the mobile phase, Eq. (1) (g/L)
c^{Init}	initial concentration of solute in column, Eq. (2) (g/L)
c^{inj}	injected concentration of solute, Eq. (3) (g/L)
D	column diameter (cm)
D_{ap}	apparent dispersion coefficient, Eq. (9) (m ² /s)
F	phase ratio, Eq. (1) (–)
L	length of column (cm)
N	number of theoretical plates (–)
q	concentration of solute in the stationary phase, Eq. (1) (g/L)
q_{si}	saturation capacity of site i in adsorption isotherm, Eq. (6) (g/L)
t_0	retention time of a non retained component (min)
t	time (min)
t^{inj}	injection time, Eq. (3) (min)
$t^{\text{inj,crit}}$	critical injection time regarding erosion of injection concentration, Eq. (13) (min)
t_R	retention times (min)
u	velocity of mobile phase Eq. (1) (cm/min)
$u_{\text{ads}}(c)$	velocity of concentration c in adsorption front (cm/min)
u_{shock}	velocity of a shock, Eq. (4) (cm/min)
$u_{\text{wave}}(c)$	velocity of concentration c in a simple wave, Eq. (5) (cm/min)
V^{inj}	injection volume (mL)
\dot{V}	volumetric flowrate (mL/min)
x	axial position in column (cm)
ε	total column porosity (–)

Acknowledgements

The financial support of the German Science Foundation (SFB 578, C2), Fonds der Chemischen Industrie and Schering AG is gratefully acknowledged.

References

- [1] G. Guiochon, S. Golshan-Shirazi, A. Katti, Fundamentals of Preparative and Nonlinear Chromatography, Academic Press, New York, 1994.
- [2] G. Guiochon, B. Lin, Modelling For Preparative Chromatography, Academic Press, Amsterdam, 2003.
- [3] G. Helfferich, G. Klein, Multicomponent Chromatography, Marcel Dekker, New York, 1970.

- [4] H.K. Rhee, R. Aris, N.R. Amundson, *Proc. R. Soc. Lond., Phil. Trans.* 267 (1970) 419.
- [5] H.K. Rhee, R. Aris, N.R. Amundson, *First-order Partial Differential Equations*, Prentice-Hall, Englewood Cliffs, New Jersey, vol. I, 1986, and vol. II, 1989.
- [6] F.G. Helfferich, P.W. Carr, *J. Chromatogr.* 629 (1993) 97.
- [7] F.G. Helfferich, R.D. Whitley, *J. Chromatogr. A* 734 (1996) 7.
- [8] F.G. Helfferich, *J. Chromatogr. A* 768 (1997) 169.
- [9] S.J. Allen, G. McKay, J.F. Porter, *J. Colloid Interface Sci.* 280 (2004) 322.
- [10] M. Mazzotti, G. Storti, M. Morbidelli, *J. Chromatogr. A* 769 (1997) 3.
- [11] C. Migliorini, M. Mazzotti, M. Morbidelli, *J. Chromatogr. A* 827 (1998) 161.
- [12] E. Glueckauf, *Proc. R. Soc. Lond.* (1946) 1302.
- [13] K. Klamer, D.W. Van Krevelen, *Chem. Eng. Sci.* 7 (1958) 197.
- [14] T. Vermeulen, M.D. LeVan, N.K. Hiester, G. Klein, in: R.H. Perry, D.W. Green, J.O. Maloney (Eds.), *Perry's Chemical Engineers' Handbook*, sixth ed., Mc Graw Hill, New York, 1984 (Section 16).
- [15] S. Brunauer, *The Adsorption of Gases and Vapours*, Oxford University Press, London, 1944, 150.
- [16] C.H. Giles, T.H. Mac Ewan, S.N. Nakhwa, D. Smith, *J. Am. Chem. Soc.* (1960) 3973.
- [17] A. Seidel-Morgenstern, G. Guiochon, *Chem. Eng. Sci.* 48 (1993) 2787.
- [18] M. Diack, G. Guiochon, *Anal. Chem.* 63 (1991) 2608.
- [19] A.P. Tudge, *Can. J. Phys.* 39 (1961) 1611.
- [20] T.L. Hill, *Introduction to Statistical Thermodynamics*, Addison-Wesley, Reading, MA, 1960.